Desalination and Water Treatment
www.deswater.com

doi: 10.5004/dwt.2018.21815

104 (2018) 83–90
February

Effects of polyacrylamide molecular weight on the effectiveness of sludge-recycling enhanced flocculation

Jia Zhu[a], Wei Wei[a,b,*], Chaosheng Zhang[b,c], Hongwei Rong[b,c], Yongfeng Cao[b]

[a]*Department of Building and Environmental Engineering, Shenzhen Polytechnic, Shenzhen, China, Tel./Fax: +86 13266518787; emails: weiweihit@hotmail.com (W. Wei), 7566874@qq.com (J. Zhu)*
[b]*School of Civil Engineering, Guangzhou University, Guangzhou, China, emails: gdzcs@126.com (C. Zhang), hwrong@gzhu.edu.cn (H. Rong), 398213541@qq.com (Y. Cao)*
[c]*Key Laboratory for Water Quality and Conservation of the Pearl River Delta, Ministry of Education, Guangzhou, China*

Received 23 July 2017; Accepted 9 December 2017

ABSTRACT

Although synthetic polymeric organic compounds have been widely used in sludge-recycling enhanced flocculation (SEF) process as the coagulant aid, effects of their molecular weight (MW) on strengthening ability and floc characteristics variation of SEF, that is, floc recovery ability, floc morphology structure and distribution, remained unclear. In this study, those effects under two colloidal destabilization mechanisms, namely electrostatic patch (EP) and near charge neutrality (NCN), in kaolin colloidal system and humic acid–kaolin colloidal system were investigated using response of SEF and traditional flocculation (TF) to polyacrylamide (PAM) with various MW. Results showed that when PAM with MW of 6 and 12 million Da was chosen, compared with TF, residual turbidity of SEF decreased by 21.45% and 27.72%, respectively, in system I, EP; –7.50% and 13.20%, respectively, in system I, NCN; 12.86% and 9.38%, respectively, in system II, EP and –98.46% and 2.10%, respectively, in system II, NCN. In most cases, the fractal dimension of SEF floc was higher than that of TF floc. And SEF could not reduce frequency of small floc, which is not beneficial to the strengthening ability exertion of SEF. However, when using PAM with MW of 18 and 20 million Da, SEF could significantly reduce the frequency of small floc, and the fractal dimension of SEF floc was lower than that of TF floc. SEF residual turbidity of PAM with 18 and 20 million Da MW decreased by 22.21% and 22.89%, respectively, in system I, EP; 21.61% and 32.19%, respectively, in system I, NCN; 33.99% and 35.29%, respectively, in system II, EP and 18.28% and 28.15%, respectively, in system II, NCN. These findings suggest that PAM with high MW and EP status was more beneficial for SEF to exhibit the strengthening ability to TF than PAM with low MW and NCN status. In addition, the recovery factor of TF floc was larger than 1, while sludge-recycling exerted a flocculation enhancement role. This suggested that the recovery ability of broken flocs had definite indication effect on exertion of SEF strengthening ability.

Keywords: Polyacrylamide; Molecular weight; Sludge recycling; Floc formation mechanism; Floc morphology

1. Introduction

Sludge-recycling enhanced flocculation (SEF) is a highly efficient water treatment technology widely used in the treatment of heavy metal wastewater, organic wastewater, domestic wastewater and potable water. A key feature of this process is the circumfluence of the sludge formed by settled floc to the forepart of the flocculation reaction, which improves the particle collision efficiency by increased sludge concentration [1,2], and sufficiently utilizes the residual flocculation ability of matured floc [3]. In many cases, the purification ability of SEF is not greater than the traditional

* Corresponding author.

flocculation (TF) process, which is mainly because recycling of sludge formed by settled floc leads to breakage of flocs, leading to the formation of a large amount of destabilized colloidal particles (under charge neutralization condition) or amorphous sediments of metal hydroxide salt (sweep flocculation). These substances under certain operating conditions are less likely to be reaggregated [4–6]. Therefore, polymer is generally added as coagulant aid in SEF-like process, which containing structural design of sludge circumfluence, to improve effluent water quality [7–10].

Since macromolecular polymeric organics have long-chain molecular structure, it adsorbs and bridges colloidal particles to accelerate the flocculation process in water treatment, resulting in the formation of flocs with large size and high density and thereby increasing floc settlement speed. Additionally, longer molecular chains can have strong contact between particle surfaces for effective adsorption and bridging. Thus, a long-chain organic polymer is usually more effective than the short-chain organic polymer with low molecular weight (MW) [11–13]. In addition, colloidal surface should have adequate space to effectively connect the long chain with other particles. Therefore, the dosage of polymeric substance could not be excess; otherwise, it can cause the coating of colloidal surface with polymers without adequate free space, leading to colloidal protection effect [14].

When adding proper dosage of polymer coagulant aid in TF, the floc is formed with a structure characterized by a long-chain molecule as skeleton with a large number of colloidal particles adsorbed on the surface. In SEF process, the settled floc is recycled in raw water or at rapid mixing stage. Under the effect of relatively high hydraulic shear force or mechanical mixing action, long-chain molecular skeleton of floc breaks. The extent of molecular chain breakage is stronger at higher shear intensity and for longer molecular chain [15,16]. Consequently, structure and distribution between floc of SEF and TF are significantly different, resulting in differences in final effluent water quality.

Although several studies have investigated about utilizing polymer in SEF, they mainly focus on final effluent water quality. Only limited studies have focused on colloidal destabilization mechanism and corresponding floc characteristics. Consequently, there is a significant gap in knowledge on the strengthening mechanism of SEF when adding polymer. The focus of this study is primarily on the effects of MW of PAM as representative polymer on the strengthening ability of SEF and floc characteristics. Using raw water prepared by kaolin and humic acid–kaolin as colloidal system, effects of polymer MW on residual turbidity, floc growth, morphology and distribution have been investigated under two colloidal destabilization mechanism conditions, including electrostatic patch (EP, relatively good coagulation effect could be acquired in this state, though colloidal particles need to refill large amount of hetero charge to reach complete charge neutralization [17–19]) and near charge neutrality (NCN, the definition is that although mark of colloid surface charge has not changed yet, it has already been close enough to the state of complete charge neutralization). Furthermore, SEF floc formation mechanism in the presence of long-chain organic polymer is discussed. Experiments were also conducted to test re-flocculation after broken (RAB) of SEF and TF flocs to investigate the recovery ability.

2. Materials and methods

2.1. Experimental setup

A floc imaging system similar to that of Wei et al. [20] was used in this study. The system included a rectangular coagulation reactor with an effective volume of 12 L (20 cm × 20 cm × 40 cm), and a programmable stirring propeller (IKA, Eurostar100, Germany) with a stainless steel blade of 100 mm × 80 mm × 2 mm. The distance between the blade and the bottom was 5 cm. The images were acquired using a high-resolution industrial camera (1,392 × 1,040 pixel, MV-VS141, Xi'an Microvision, China) and high-resolution lens (10 million pixels, LM25JC10M, Kowa, Japan).

2.2. Materials

Coagulant aid used in this study was mainly commercially available polyaluminum chloride (PACl) with 30% of Al_2O_3 content, 40%–90% of basicity, and pH of 3.8. A 87.43 mg/L stock solution (calculated based on Al^{3+} concentration) was prepared by dissolving PACl using deionized water. According to the Ferron timed complex colorimetry analysis results, Al_a, Al_b and Al_c in coagulant aid were 15.71%, 63.43%, and 20.86%, respectively.

Anionic polyacrylamides (SNF Floerger, France) with MWs of 6 (AN934BPM, 30% mole ratio of anion content), 12 (AN926SHU, 25% mole ratio of anion content), 18 (AN926SH, 25% mole ratio of anion content), and 20 (AN934VHM, 30% mole ratio of anion content) million Da were selected as representative long-chain polymer electrolytes. PAM was diluted to 0.1% solution using deionized water, and used within 24 h.

2.3. Preparation of colloidal system

Kaolin stock solution was prepared by dispersing 100 g kaolin clay (AR, Tianjin Damao Chemical Reagent Factory, Tianjin, China) in 1 L deionized water, and stirring it rapidly at 1,000 rpm for ~2 h. The pH was adjusted to 8.5 using 0.5 mol/L NaOH solution. After standing overnight, the upper layer of the suspension was collected and used as the kaolin stock solution. The particle size distribution of the suspension was measured by a laser particle size analyzer (S3500, Microtrac, USA) ranged from 1 to 20 μm.

Humic acid stock solution was prepared by dissolving 15 g sodium humate (AR, Aladdin Shanghai Biochemical Technology LLC, Shanghai, China) in 1 L deionized water, and the pH value was adjusted to 8.5 using 0.5 mol/L NaOH (GR, Shanghai Engineering Group, imported, Shanghai, China) under rapid stirring. The solution was stirred continuously for 1 h, after which the solution was centrifuged and its upper layer was collected in a reagent bottle. The insoluble bottom ballast was elutriated and centrifuged for multiple times and the upper layer solution was poured into the reagent bottle.

Two suspension colloidal systems used in experiments were prepared by mixing kaolin stock solution and sodium humate stock solution in tap water. For kaolin suspension colloidal system (system I), 50 mL kaolin stock solution was diluted to 75 L using tap water. The alkalinity was adjusted to ~120 mg/L (calculated as $CaCO_3$) by 0.5 mol/L $NaHCO_3$ (AR, Tianjin Kemiou Chemical Reagent Co., Ltd.,

Tianjian, China), while the pH value was adjusted to around 7.9 ± 0.05 by 0.5 mol/L NaOH solution (GR, Shanghai Shanhai Gongxuetuan No. 2 Experiment Factory, Shanghai, China) or 2 mol/L HCl (GR, Guangzhou Donghong Chemical Factory, Guangzhou, China). For humic–kaolin suspension colloidal system (system II), 25 mL humic stock solution was added into system I. System II was stirred uniformly and kept overnight to reach adsorption equilibrium of humic acid.

The turbidity of two systems was in the range of 40–43 NTU measured by a portable turbidimeter (2100Q, Hach, USA). The testing water temperature was between 20.8°C and 27.9°C. The zeta potentials of system I and II measured by a zeta potential detector were found to be –26.67 and –30.80 mV, respectively (90 Plus Zeta, Brookhaven, USA).

2.4. Experimental method

First, coagulant dosage test was conducted to determine EP and NCN destabilization mechanisms of two colloidal systems. For coagulant dosages of 1.46 and 2.73 mg/L, the respective zeta potential of system I was –12.64 and –1.11 mV, while the respective residual turbidity values were 6.39 and 2.22 NTU. According to the definition of the state EP and NCN mentioned above, these dosages were determined as the EP and NCN coagulant dosages in system I. Similarly, when coagulant dosages were 3.64 and 7.29 mg/L, zeta potentials of system II were –12.45 and –1.95 mV, respectively, whereas the residual turbidity values were 9.46 and 5.34 NTU, respectively. These were determined as the EP and NCN coagulant dosages in system II.

For TF, a pre-determined dosage of coagulant was added and rapidly stirred at 300 rpm for 1.0 min. 0.20 mg/L PAMs with different MW (6, 12, 18, and 20 million Da) were added at the beginning of slow stirring stage (70 rpm). The system was stirred for 15 min and left to settle for 10 min before collecting water samples at 3 cm underwater for turbidity determination. In this study, due to the difficulty in controlling the sludge concentration, the amount of settled sediments in single TF test was used as the measurement scale to avoid large errors between the control trials. One-time dosing of sludge produced by a single TF test was defined as "single-dosage." In control group, the operating condition of SEF was similar to that of TF, except that the settled floc was added at one time in raw water before coagulant addition, followed by stirring at 300 rpm for 1 min.

A 60 s rapid breakage stage at 300 rpm followed by a 15 min recovery phase at 70 rpm and a 10 min settlement with no mixing were performed to test the ability of flocs to resist rupture and re-flocculation of broken flocs.

2.5. Image acquisition and analysis

Image acquisition parameters were set as two photographs per min for rapid stirring stage and one photograph per min for slow stirring stage. Floc particle count, and morphological parameters such as perimeter, area, and diameter were analyzed by a professional image processing software IPP 7 (Image Pro Plus 7.0, Media Cybernetics, USA) using grayscale pictures of the floc. The average of all the floc diameter values in each picture was denoted as the average floc particle size for the corresponding moment.

The perimeter-based fractal dimension reflected the irregular geometry of floc two-dimensional projection, with fractal dimension value ranging from 1 (regular, and spherical) to 2 (irregular, serrated or linear, and non-spherical). Perimeter-based fractal dimension increases since the perimeter grows more rapidly than Euclidean geometry when the projected area of one fractal floc increases [21–24]. Scatterplot of log$A$-log$P$ was drawn according to Eq. (1), and the linear portion of the scatterplot was selected and fitted to obtain the slope. The fractal dimension value for the corresponding moment was calculated by multiplying the slope by 2.

$$A \propto P^{2/D_{pf}} \tag{1}$$

where D_{pf}, A, and P denote perimeter-based fractal dimension, projected area of the floc, and the perimeter of flocs.

The floc breakage factor and recovery factor are defined by Eqs. (2) and (3):

$$B_f = \frac{d_a - d_b}{d_a} \tag{2}$$

$$R_f = \frac{d_c}{d_a} \tag{3}$$

where d_a, d_b, and d_c are the steady-state floc size before breakage, after breakage, and after recovery phase, respectively [20].

3. Results

3.1. Removal of residual turbidity

Residual turbidity in system I and system II under EP and NCN state is shown in Fig. 1. As evident in Fig. 1, total residual turbidity shows a decreasing trend with increasing PAM MW, indicating that PAM with larger MW is beneficial for the residual removal.

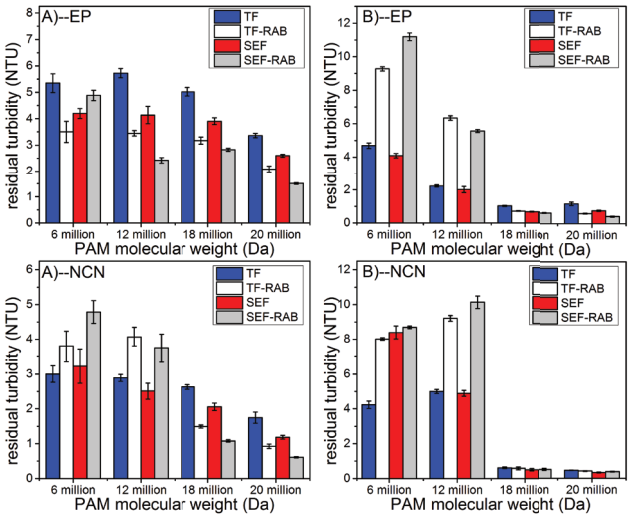

Fig. 1. Residual turbidity at different PAM molecular weight (dosage, 0.20 mg/L): (A) system I and (B) system II.

Meanwhile, MWs also had significant impacts on strengthening the behavior of SEF. Specifically, for system I (Fig. 1(A)), residual turbidity in SEF reduced by 21.45%–27.72% compared with TF under EP state. In addition, TF-RAB and SEF-RAB generally showed reinforcement impacts compared with the corresponding TF and SEF. Only for MW of 6 million Da, the residual turbidity of SEF-RAB was higher than that of SEF. Under NCN state, residual turbidity of SEF increased by 7.50% when MW was 6 million and did not show reinforcement on TF. Further, the residual turbidity of TF-RAB and SEF-RAB both increased significantly. However, when MW was 12 million Da, the residual turbidity of SEF was 13.2% lower than that of TF, although residual turbidity of RAB of SEF and TF increased significantly. And when MWs were 18 and 20 million Da, SEF showed reinforcement impact on TF. The residual turbidity decreased 21.61% and 32.19%, respectively, and RAB of both also decreased their residual turbidities of corresponding TF and SEF.

For system II, adding PAM could make SEF play reinforcement role in EP state (Fig. 1(B)). When MW of the selected PAM was 6 and 12 million Da, the corresponding residual turbidity in both SEF-RAB and TF-RAB increased significantly, while the corresponding residual turbidity of SEF only reduced by 12.86% and 9.38%, respectively, than that of TF. For MWs of 18 and 20 million Da, the respective residual turbidity of SEF reduced by 33.99% and 35.29% along with the significant decrease in residual turbidity of both RAB. Similar to system I in NCN state, when system II was in NCN state, MWs of 6 and 12 million Da were disadvantageous for the exertion of reinforcement effect by SEF. The residual turbidity of SEF increased by 98.46% when MW was 6 million Da, and did not enhance the flocculation. Similarly, the residual turbidity of SEF only reduced by 2.10% when MW was 12 million Da. When MWs were 18 and 20 million Da, the corresponding residual turbidity of SEF decreased by 18.28% and 28.15%, respectively, and showed a significant reinforcement impact.

In summary, PAM with a lower MW is unfavorable for reinforcement of SEF, while higher MW could reduce residual turbidity, and guarantee the reinforcement impact of settled sludge on TF. Variation of effluent efficiency of TF-RAB compared with TF could not fully reflect reinforcement of SEF on TF, which was different from on the previous conclusion when "no PAM added" [20]. In addition, results also imply that compared with NCN state, EP state is more favorable for reinforcement of SEF on TF.

3.2. Floc growth with different PAM molecular weight

Influence of PAM MW on floc growth and the corresponding floc factors under EP and NCN conditions in two water distribution systems are shown in Figs. 2 and 3, respectively.

According to Fig. 2 for system I, floc growth of TF and SEF was inhibited to some extent, for example, in EP state (Fig. 2(A)), when MWs of PAM were 18 and 20 million Da. For 18 million Da, the floc particle sizes in TF and SEF at the end of stirring were 102.89 and 114.25 μm, respectively. This was significantly lower than floc particle size of 150.86 and 213.36 μm when MW was 12 million Da. However, large MW could reduce the breakage properties and increase the recovery ability of floc in SEF and TF. Under two charge state,

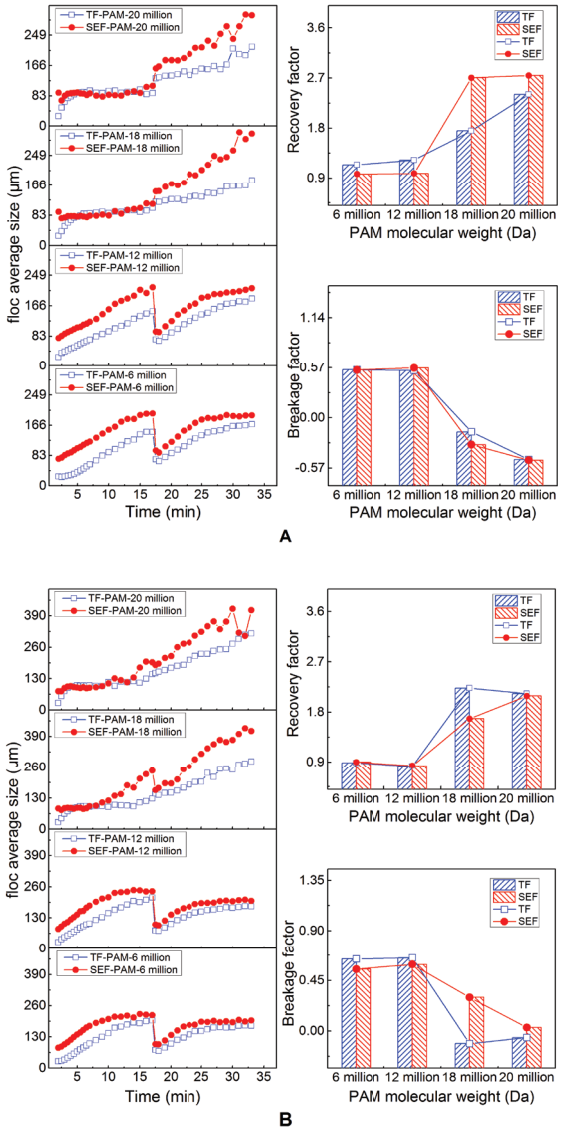

Fig. 2. Floc growth and its factors for system I at different PAM molecular weight: (A) state of EP, and (B) state of NCN.

the breakage factors of floc decreased gradually along with the increase in MW, while the recovery factors gradually increased. When PAM MW was higher than 18 million Da, floc recovery factors of SEF and TF were significantly larger than 1. It was also found that floc recovery property of SEF in EP state was higher than that in NCN state.

For system II, relatively high MW of PAM inhibited floc growth when system was in EP state (Fig. 3(A)). In contrast, the inhibition of PAM with higher MW to floc growth was not significant when the system was in NCN state (Fig. 3(B)). For MW of 18 million Da, floc growth was rapid with larger floc particle size for these two flocculation types. The floc recovery ability of TF and SEF after adding PAM with higher MW was significantly higher than that with lower MW. Besides, the floc breakage factor gradually decreased with increasing MW in EP state, whereas it showed an increasing trend in NCN state. Although the recovery factor remained low, this did not affect the reinforcement of SEF on TF. This can be

because the large flocs under this condition consisted of large amount of easily exfoliated crushed clusters, which still had a relatively good settleability.

According to the residual turbidity results for both system I and system II, SEF could exert its reinforcement effect on TF if the TF floc recovery factor was larger than 1. This phenomenon indicated that the recovery property of broken flocs could indicate the exertion of reinforcement effect of SEF. However, in some cases when using PAM with relatively low MW (6 and 12 million Da), even if the residual turbidity of TF-RAB increased relative to that of TF and the recovery factor of TF floc was lower than 1 indicating a weak recovery ability, SEF still exerted reinforcement effect to TF. For example, the floc recovery factor was only 65.8% when 12 million Da PAM was added in system II in NCN state. This is because of the adsorption of a large number of small particles, which could not accomplish self-coagulation after breakage by the bridging mechanism, introduced by addition of PAM in corresponding SEF reaction with relatively low TF floc recovery factor. This indicated that addition of high-molecular polymer could have favored the exertion of reinforcement effect of SEF.

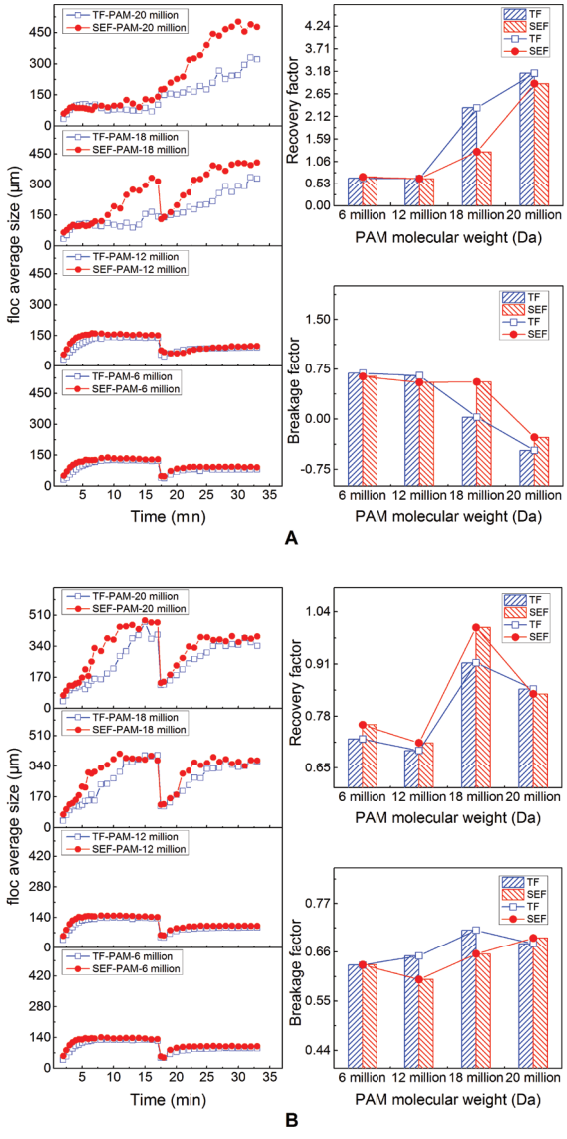

Fig. 3. Floc growth and its factors of system II at different PAM molecular weight: (A) state of EP and (B) state of NCN.

3.3. Floc morphology at the end of stirring with different PAM molecular weight

The influence of PAM addition of different MWs on floc fractal dimension of TF and SEF at the end of stirring is shown in Fig. 4.

According to Fig. 4, floc fractal dimension generally decreased with the increase of PAM MW in total. When system I was in EP state, floc fractal dimension of SEF was lower than that of TF. However, the floc fractal dimensions of SEF in NCN state for 6 and 12 million Da PAM were 1.314 and 1.296, respectively, which are higher than that of 1.289 and 1.288, respectively, for TF floc. For the addition of 18 and 20 million Da, the floc fractal dimensions of SEF were 1.255 and 1.252, respectively, which are lower than that of 1.280 and 1.263, respectively, of TF floc. The phenomenon of system I in NCN state also appeared in system II in EP state and NCN state (Fig. 4(B)). According to the definition of perimeter-based fractal dimension, floc morphology with lower fractal dimension was closer to sphere, which is more favorable to floc settlement to achieve a better removal of turbidity [21]. Above results show that adding PAM with higher MW is more favorable for SEF to form more advantageous floc structure compared with the morphology of TF floc.

3.4. Floc distribution with different PAM molecular weight

The floc distribution of SEF, TF, and TF-RAB at the end of stirring for PAM with lower MW (6 million Da) and higher MW (18 million Da) in two charge states is shown in Figs. 5 and 6, respectively. As evident in Figs. 5 and 6, adding PAM with MW of 18 million Da could significantly reduce the total frequency of floc compared with MW of 6 million Da for the same dosage. It is generally recognized that for flocs with smaller size implies lower settlement rate for similar density [25,26], and floc size distribution at the end of stirring has an impact on effluent water quality after coagulation, especially

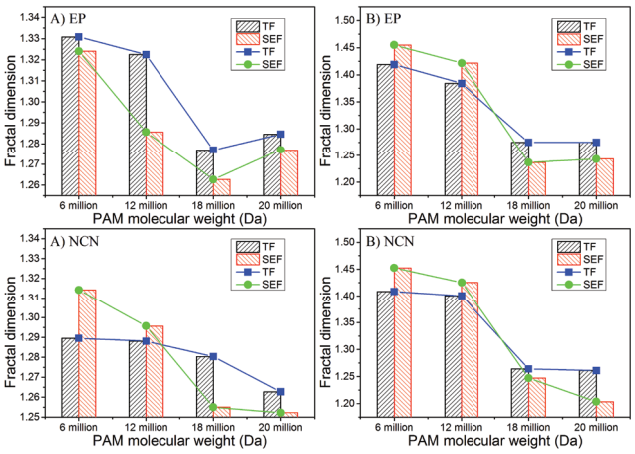

Fig. 4. Floc fractal dimension of TF and SEF at different PAM molecular weight: (A) system I and (B) system II.

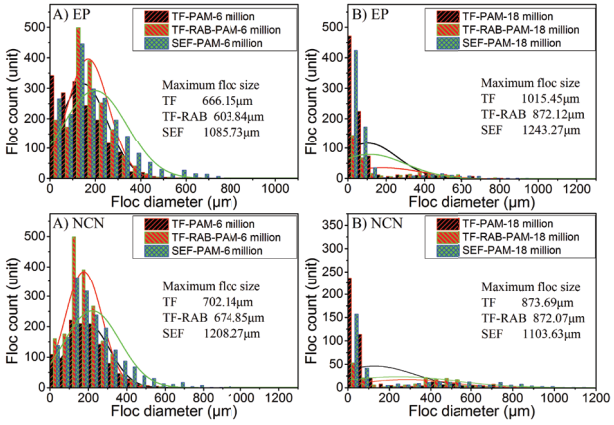

Fig. 5. Floc size distribution in system I for different PAM molecular weight: (A) molecular weight 6 million Da and (B) molecular weight 18 million Da.

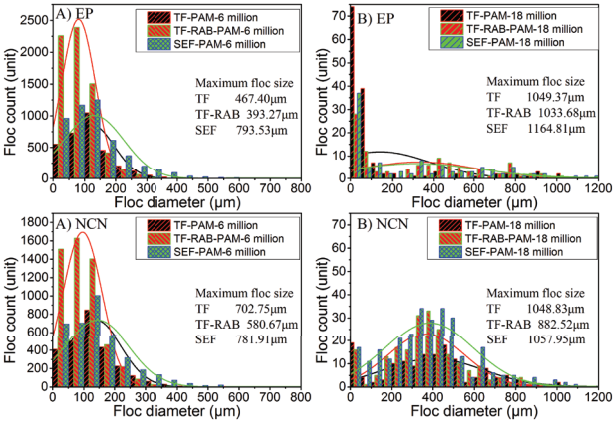

Fig. 6. Floc size distribution in system II for different PAM molecular weight. (A) Molecular weight 6 million Da and (B) molecular weight 18 million Da.

the presence of small floc size commonly leads to ineffective turbidity removal. This study mainly concerned with frequency of flocs with diameter smaller than 50 μm for the investigation of floc size distribution.

For system I (Fig. 5), in EP state, small floc frequencies (<50 μm) of TF-RAB with PAM MWs of 6 and 18 million Da were 196 and 145, respectively, which are significantly lower than those of TF, that is, 342 and 472, respectively. When adding PAM with MW of 18 million Da (Fig. 5(B)), the reduction amplitude was larger than that for 6 million Da (Fig. 5(A)). Meanwhile, when PAM MW was 6 and 18 million Da, the frequencies of SEF small floc were 226 and 424, respectively, which also significantly lower than that of TF. In NCN state, when PAM with MW of 6 million Da was added, the small floc frequencies of TF-RAB and SEF were 161 and 138, respectively, which are slightly higher than that of TF (109). This indicates that activity of broken flocs was not strong. When PAM with MW of 18 million Da was added, the small floc frequencies of TF-RAB and SEF were 53 and 157, respectively, which are significantly lower than that of TF (237).

For system II, when adding PAM with MW of 6 million Da (Fig. 6(A)), the small floc frequencies of TF, TF-RAB, and SEF in EP state were 552, 2,261, and 959, respectively, while they were 412, 1,512, and 695, respectively, in NCN state. The TF-RAB and the corresponding SEF led to significant increase in small floc frequency. When adding PAM with MW of 18 million Da (Fig. 6(B)), small floc frequencies of TF, TF-RAB, and SEF in EP state were 74, 28, and 37, respectively, whereas they were 19, 16, and 17, respectively, in NCN state. As such, TF-RAB and SEF reduced the frequency of small flocs.

Floc RAB indicated the ability of re-flocculation after floc breakage, while frequency of residual small floc after re-flocculation suggested the activity of broken floc from another perspective. When adding PAM with higher MW, small floc frequencies of SEF and TF-RAB were lower than those of TF, indicating that the adsorption ability of small flocs was better after floc breakage, showing high activity. While adding PAM with lower MW, small floc frequency of SEF and TF-RAB increased for most cases, though the adsorption of small flocs was inefficient after floc breakage with low activity, which could result in the deterioration of effluent water quality.

It was also found that SEF had a wide range of particle size than that of TF, that is, increase in the distribution uniformity, and floc uniformity due to the addition of PAM with higher MW was better than that for lower MW.

4. Discussion

It is commonly thought that long-chain molecular structure of PAM could strongly adsorb aqueous particles, though the molecular chain would break under the action of high hydraulic shear force or mechanical stirring. The rupture degree is considered to be higher with higher shear intensity. However, it would not generally lead to disintegration of molecular chain to a monomer [27]. Based on this knowledge, SEF floc formation mechanism in the presence of long-chain molecules could consist of the following steps (Fig. 7):

① When coagulant is added into the raw water with a large number of dispersed colloidal particles, ② the primary aggregates are formed in TF reaction. ③ After polymer dosing, the primary aggregates are adsorbed on molecular chain through bridging mechanism to form flocs with large size, but with relatively open floc morphology. ④ After adding sediments formed by TF, under strong stirring, molecular chain is broken in a large scale to yield a large number of micro flocs carrying short chain. After adding coagulant aid, ⑤ raw water colloids could form primary aggregates, while the active sites are supplemented on surface of micro floc and clustered with primary aggregates. When PAM is added again, ⑥ micro flocs with raw water colloid and primary aggregates absorbed both are absorbed on long molecular chain of the newly added PAM.

In the reaction of TF, large open-structure flocs were formed by the primary aggregates bridging to the molecular chain of the polymer. Because of a reduction in particle concentration resulting from rapid adsorption of the primary aggregates on the polymer, the collision efficiency decreases; therefore, many primary flocs cannot effectively collide. It is easier to form a large number of small flocs that are not easily settled, which is not conducive to the solid–liquid separation process.

Through the six steps mentioned above, the SEF floc had significantly large size, dense structure, and prior

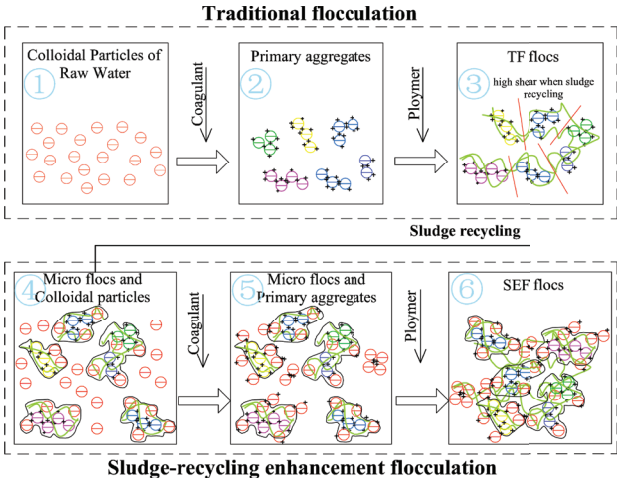

Fig. 7. Schematic diagram of SEF floc formation in the presence of bridging effect by long-chain molecules.

morphology. The key operation of sludge recycling increased the solid concentration, while the powerful mechanical stirring or hydraulic shear force responsible for cutting off the long-chain molecular and matured flocs from settled sludge and the addition of new agent also played important roles. The former helps the increase of particle amount which is attributed to the raise of collision frequency between particles. Since the active sites on the surface of micro flocs were occupied with the short-chain skeleton, sludge recycling alone is not adequate to destabilize the colloids in raw water, although the micro flocs could adsorb a fraction of it. Therefore, the new coagulant needs to be added. After polymer addition, the flocculation tank became a reaction system consisting of primary aggregates, micro flocs with plenty of active sites and long-chain molecular. The flocculation occurs using the agglomerate cores function of micro flocs and the strong adsorption of polymer. In this process, micro flocs adsorb primary aggregates, and can be connected to long-chain molecular. This leads to the multi-level structure of SEF flocs with larger size than that of TF. Micro flocs could fill up the space which originally belongs to TF flocs resulting in a superior morphology. Furthermore, some tiny particles or stable colloids that cannot be settled in TF can remain in the multi-level structures. This leads to decreased frequency of small floc with diameter smaller than 50 μm.

The polymer MW reflects the development length of the molecular chain. At an appropriate pH in aqueous solution, a stretched chain with a higher MW has a greater radius of gyration and intrinsic viscosity, and can adsorb more microflocs and primary aggregates to create more space for the cladding of tiny particles or stable colloids. During the continuing flip and distortion, the configuration of SEF floc can be easily changed to a denser structure and lower fractal dimension morphology. Thus, SEF with a high MW has a greater effect on TF than SEF with low MW, as can be seen in the results of this study. In addition, the ionic nature and charge density of a polymer also influences the aggregation process. For negatively charged fine particles, a polymer with a cationic addition can induce the charge neutralization mechanism of flocculation [28], while in an anionic polymer, bridging is the primary aggregation mechanism [29]. The increasing cationic density may help colloidal particles reach the electrically neutral state more quickly, while the increasing anionic density increases the electrostatic repulsion between the kaolinite particles and the anionic polymer, which may lead to the avoidance of kaolinite particle restabilization because of excessive polymer adsorption driven by strong electrostatic attraction [13]. In the two kaolin suspension colloidal systems, the different MWs of the anionic PAM used in this study only served as the representative material playing the bridging role. However, after coagulant addition, the electrostatic adsorption between the positive surface charge of the primary aggregates or microflocs and the anionic of the PAM is of significance in the formation of floc as well. In SEF, when considering the ionic nature and charge density of coagulant aids, floc formation becomes more complex and experiments designed similarly to those reported here should be conducted to investigate in more detail floc formation rules using different types of polymers with a wider range in charge density.

The charge states of the reactor system after adding coagulant are another important factor responding to SEF performance in this study. Our findings showed that an EP state was more beneficial for SEF in strengthening the ability of TF than an NCN state. According to the explanation of the EP effect reported by Ye et al. [19], static clusters with a strong positive charge are mainly produced by the Al_b (Al_{13}) constituent, and "static cluster/colloid surface" is the flocculation feature of H PACl (greater than 75% Al_b), which means the flocculation does not require full-charge neutralization. But for the L PACl (greater than 90% Al_a), the hydrolyzates of Ala adsorbed or deposited on the colloid surface form static clusters with a weak charge creating a fragile "static cluster/static cluster" structure. In this study, although polymer materials were added to make bridging the main aggregation mode, the primary aggregate part exposed to the water body that still possesses its original characteristics under different charge states should be noted in the SEF. The NCN state means that there is a higher PACl dosage than in the EP state. Considering the components of the PACl used, this may increase the number of "static cluster/static cluster" structures which can lead to an increased risk of microflocs stripping from SEF flocs.

5. Conclusions

SEF technology in the presence of polymer long-chain bridging effects was primarily investigated in two colloidal systems. The experiments to investigate the influence of PAM with different MW on SEF effectiveness and performance were conducted based on strict trials. From perspective of effluent water quality, SEF could not guarantee to exert reinforcement effects on TF in NCN state of kaolin colloidal system, and EP and NCN state of humic acid–kaolin colloidal system, when adding PAM with MW of 6 and 12 million Da. In contrast, adding PAM with MW of 18 and 20 million Da reduced residual turbidity, and guaranteed reinforcement action of SEF on TF. From the perspective of floc growth characteristics, morphology, and distribution, recovery ability of floc was poor in most circumstances, when adding PAM with lower MW. Comparing with TF, SEF could not reduce small floc frequency, resulting in undesired morphology of the

formed floc. This was unfavorable for floc settlement and turbidity removal, while adding PAM with higher MW showed the opposite effect. In the context of fluctuating water quality in practical systems, this study suggests to utilizing PAM with higher MW to guarantee stable reinforcement performance of SEF process. In addition, SEF could exert reinforcement effect on TF in all TF-SEF control test, provided that the recovery factor of TF floc was larger than 1. This indicates that recovery ability of broken flocs plays a significant indicative role in the exertion of SEF reinforcement. So, this study also suggests that floc recovery factor could be used as a control parameter for process effectiveness in practical application of SEF.

Acknowledgments

The work was financially supported by the National Natural Science Foundation of China (Number: 51478274), Foundation for Distinguished Young Talents in Higher Education of Guangdong, China (Number: 2014kqncx105) and Opening Fund of Key Laboratory for Water Quality and Conservation of the Pearl River Delta, Ministry of Education (Number: 201702).

References

[1] Z. Zhou, Y. Yang, X. Li, W. Wang, Y. Wu, C. Wang, J. Luo, Coagulation performance and flocs characteristics of recycling pre-sonicated condensate sludge for low-turbidity surface water treatment, Sep. Purif. Technol., 123 (2014) 1–8.
[2] L. Qi, H. Liang, Y. Wang, G.B. Li, Integration of immersed membrane ultrafiltration with the reuse of PAC and alum sludge (RPAS) process for drinking water treatment, Desalination, 249 (2009) 440–444.
[3] B. Xi, Y. Zhao, L. Zhang, X. Xia, Z. Luan, X. Peng, W. Lv, Return chemical sludge employed in enhancement of phosphate removal from wastewater, Desal. Wat. Treat., 52 (2014) 6639–6647.
[4] W. Yu, J. Gregory, L. Campos, G. Li, The role of mixing conditions on floc growth, breakage and re-growth, Chem. Eng. J., 171 (2011) 425–430.
[5] M.A. Yukselen, J. Gregory, The reversibility of floc breakage, Int. J. Miner. Process., 73 (2004) 251–259.
[6] M.A. Yukselen, J. Gregory, The effect of rapid mixing on the break-up and re-formation of flocs, J. Chem. Technol. Biotechnol., 79 (2004) 782–788.
[7] B. Wang, Z. Chen, J. Zhu, J. Shen, Y. Han, Pilot-scale fluoride-containing wastewater treatment by the ballasted flocculation process, Water Sci. Technol., 68 (2013) 134–143.
[8] T.I. Yoon, C.G. Kim, Case studies on rapid coagulation processes to cope with total emission controls, Desalination, 231 (2008) 290–296.
[9] J. Huang, J. Zhu, C.S. Zhang, W. Wei, Research on conventional flocculation and loading flocculation process for zinc, copper wastewater treatment, GuangZhou Chem. Ind., 40 (2012) 1–4.
[10] M.B. Asif, N. Majeed, S. Iftekhar, R. Habib, S. Fida, S. Tabraiz, Chemically enhanced primary treatment of textile effluent using alum sludge and chitosan, Desal. Wat. Treat., 57 (2016) 7280–7286.
[11] C.S. Lee, J. Robinson, M.F. Chong, A review on application of flocculants in wastewater treatment, Process Saf. Environ., 92 (2014) 489–508.
[12] M. Razali, Z. Ahmad, M. Ahmad, A. Ariffin, Treatment of pulp and paper mill wastewater with various molecular weight of polyDADMAC induced flocculation, Chem. Eng. J., 166 (2011) 529–535.
[13] M.S. Nasser, A.E. James, The effect of polyacrylamide charge density and molecular weight on the flocculation and sedimentation behaviour of kaolinite suspensions, Sep. Purif. Technol., 52 (2006) 241–252.
[14] F. Sher, A. Malik, H. Liu, Industrial polymer effluent treatment by chemical coagulation and flocculation, J. Environ. Chem. Eng., 1 (2013) 684–689.
[15] F. Bueche, Mechanical degradation of high polymers, J. Appl. Polym. Sci., 4 (1960) 101–106.
[16] H.J. Choi, C.A. Kim, J. Sohn, M.S. Jhon, An exponential decay function for polymer degradation in turbulent drag reduction, Polym. Degrad. Stab., 69 (2000) 341–346.
[17] J. Gregory, Rates of flocculation of latex particles by cationic polymers, J. Colloid Interface Sci., 42 (1973) 448–456.
[18] Y. Cheng, R. Wong, J.C. Lin, C. Huang, D. Lee, A.S. Mujumdar, Water coagulation using electrostatic patch coagulation (EPC) mechanism, Drying Technol., 28 (2010) 850–857.
[19] C. Ye, D. Wang, B. Shi, J. Yu, J. Qu, M. Edwards, H. Tang, Alkalinity effect of coagulation with polyaluminum chlorides: role of electrostatic patch, Colloids Surf., A, 294 (2007) 163–173.
[20] W. Wei, X. Li, J. Zhu, M. Du, Characteristics of flocs formed by polyaluminum chloride during flocculation after floc recycling and breakage, Desal. Wat. Treat., 56 (2015) 1110–1120.
[21] P. Bubakova, M. Pivokonsky, P. Filip, Effect of shear rate on aggregate size and structure in the process of aggregation and at steady state, Powder Technol., 235 (2013) 540–549.
[22] W. He, J. Nan, H. Li, S. Li, Characteristic analysis on temporal evolution of floc size and structure in low-shear flow, Water Res., 46 (2012) 509–520.
[23] P.T. Spicer, W. Keller, S.E. Pratsinis, The effect of impeller type on floc size and structure during shear-induced flocculation, J. Colloid Interface Sci., 184 (1996) 112–122.
[24] M. Soos, A.S. Moussa, L. Ehrl, J. Sefcik, H. Wu, M. Morbidelli, Effect of shear rate on aggregate size and morphology investigated under turbulent conditions in stirred tank, J. Colloid Interface Sci., 319 (2008) 577–589.
[25] I. Slavik, S. Müller, R. Mokosch, J.A. Azongbilla, W. Uhl, Impact of shear stress and pH changes on floc size and removal of dissolved organic matter (DOM), Water Res., 46 (2012) 6543–6553.
[26] M. Boller, S. Blaser, Particles under stress, Water Sci. Technol., 37 (1998) 9–29.
[27] J. Yu, J.L. Zakin, G.K. Patterson, Mechanical degradation of high molecular weight polymers in dilute solution, J. Appl. Polym. Sci., 23 (1979) 2493–2512.
[28] Y. Zhou, G.V. Franks, Flocculation mechanism induced by cationic polymers investigated by light scattering, Langmuir, 22 (2006) 6775–6786.
[29] P. Mpofu, J. Addai-Mensah, J. Ralston, Investigation of the effect of polymer structure type on flocculation, rheology and dewatering behaviour of kaolinite dispersions, Int. J. Miner. Process., 71 (2003) 247–268.